Computers in Biology and Medicine 108 (2019) 234–241

Contents lists available at ScienceDirect

Computers in Biology and Medicine

journal homepage: www.elsevier.com/locate/compbiomed

Spatial remodelling of calcium release units may impair cardiac electro-mechanical function: A simulation study

Luyao Lu[a], Qianqian Zheng[a], Ling Xia[b], Xiuwei Zhu[a,*]

[a] School of Biomedical Engineering, Wenzhou Medical University, University Town, Chashan, Wenzhou, 325035, PR China
[b] Department of Biomedical Engineering, Zhejiang University, 38 Zheda Road, Hangzhou, 310027, PR China

ARTICLE INFO

Keywords:
Calcium dynamics
Heart failure
Multiscale mathematical model
Uncoupling of LCC-RyRs

ABSTRACT

Excitation-contraction coupling (E-C coupling) is thought to be based on elementary calcium release units (CRUs) in which clusters of ryanodine receptors (RyRs) localized on the sarcoplasmic reticulum (SR) are in close apposition to L-type Ca^{2+} channels (LCCs) on the transverse tubules (TTs). However, a fraction of LCC-RyR structure may be uncoupled due to the remodelling of TTs, which would tend to destroy the E-C coupling in the failing heart. Here we proposed a multiscale model of the ventricular myocyte to investigate the relationship between LCC-RyR structure and cardiac electro-mechanical function. The mathematical model consisted of a two-dimensional (2D) subcellular Ca^{2+} reaction-diffusion sub-model, a cellular electrophysiological sub-model and a cardiomyocyte contraction sub-model. The simulation results showed that the remodelling of CRU microstructure would disturb Ca^{2+} homeostasis, leading to a dyssynchronous Ca^{2+} transient, and postpone the generation of isometric force. Our study suggests that structural remodelling is an important mechanism for dysfunction of Ca^{2+} handling, cellular electrophysiology and contractility in failing heart.

1. Introduction

During an action potential (AP), transmembrane Ca^{2+} entry via depolarization-activated Ca^{2+} channels will trigger a much larger Ca^{2+} release flux from sarcoplasmic reticulum (SR), called Ca^{2+}-induced-Ca^{2+}-release (CICR), which leads to a global steep rise of Ca^{2+} concentration, i.e. $[Ca^{2+}]_i$ transient. Efficient CICR and tight excitation-contraction coupling (E-C coupling) are enabled by special subcellular structures named calcium release units (CRUs). CRUs contain two proteins, dihydropyridine receptors (DHPRs), L-type Ca^{2+} channels (LCCs) on the transverse tubules (TTs), and ryanodine receptors (RyRs) localized on the sarcoplasmic reticulum (SR). Tens of RyRs in a CRU are resembled as a cluster [1,2], activation of which will increase a local Ca^{2+} signal that is widely accepted as Ca^{2+} spark [3]. The junctional gap between SR and TTs is about 12 nm [4] and the nanometer-sized structure referred to functional grouping of LCCs and RyRs has also been called “couplon” [5].

Heart failure (HF) has become a leading cause of death with a poor prognosis, whose five-year mortality rate is about 50% [6]. Failing heart muscle cells are characterized by reduced contractility, impaired Ca^{2+} dynamics and arrhythmias. As reported, the important factors affecting Ca^{2+} cycling are alterations of ion channels and Ca^{2+} buffer proteins in the development of HF, including increased expression and/or activity of Na^+/Ca^{2+} exchange (NCX) [7], decreased SR Ca^{2+} pump activity and expression level [8,9], elevated SR Ca^{2+} leak [10], reduction in inward rectifier potassium current (I_{K1}) [11], mitochondrial Ca^{2+} overload [12], and altered glycosylation and phosphorylation of calsequestrin [13,14]. Alternatively, other work suggested that unclustered or rogue RyRs, probably due to subcellular structural remodelling, could be a candidate factor affecting Ca^{2+} cycling and triggering arrhythmia in failing heart [15–17]. Moreover, structural remodelling of TTs was found in ventricular myocytes from hypertensive failing heart [18]. During the remodelling process a portion of LCCs left their original locations, just like ‘stray LCCs’, but the RyRs remained in situ, which suggests that the tight coupling structure of couplons was destroyed. The increased spatial dispersion of TTs and uncoupled LCCs might be responsible for Ca^{2+} instability.

However, it is still unclear how the abnormal Ca^{2+} cycling, ion channel and structural remodelling affect the electro-mechanical properties of failing myocytes. In this study, we developed a multiscale mathematical model and simulated the subcellular Ca^{2+} release events, the cellular Ca^{2+} cycling and the electrophysiology and mechanics of a whole cell. The proposed model was applied to study impaired Ca^{2+} cycling, electrophysiology and contraction in heart failure, especially, to evaluate the effects of the uncoupling of LCC-RyR structure on electro-mechanical dynamics of the ventricular cells.

* Corresponding author.
E-mail address: zhuxw@wmu.edu.cn (X. Zhu).

https://doi.org/10.1016/j.compbiomed.2019.04.007
Received 5 August 2018; Received in revised form 8 April 2019; Accepted 10 April 2019

2. Methods

A multiscale mathematical model of human ventricular myocyte is developed by integrating our previous coupled model [16] and the contraction model proposed by Gentaro Iribe et al. [19]. The model consists of three parts: a two-dimensional (2D) spatial subcellular Ca^{2+} reaction-diffusion model, an electrophysiological model and a force computation model of the ventricular myocyte.

2.1. Subcellular Ca^{2+} reaction-diffusion model

In our model, a ventricular myocyte is represented by a circular cylinder with 100 μm in length and 20 μm in diameter. In each sarcomere with the length of 2 μm (l_x), CRUs are located regularly on the Z-line at intervals of 1 μm (l_y), as shown in Fig. 1(A). In a CRU, L-type channel and RyRs cluster are localized face to face and are separated by very narrow cleft. Because of the quasi-isotropic diffusion of Ca^{2+} on the transverse section [20], the 3-D model is simplified to a 2-D model in which x axis denotes the cell's longitudinal direction and y axis is along the Z-line. Fig. 1(B) shows the 2-D model of CRUs network in the healthy heart cell, where LCCs and RyRs are colocalized as a couplon in the same grid. In Fig. 1(C), due to the remodelling of TTs system in heart failing cells, some LCCs are redistributed and the corresponding RyRs are left behind. In our model, those uncoupled LCCs are randomly selected and moved away from their original sites with random distances and directions. To describe the uncoupling degree of LCCs and RyR clusters, we define a variable Un_{LCC}% as the ratio of uncoupling LCCs with RyRs to total LCCs. The Un_{LCC}% is varied from 10% to 60% to evaluate the effect of uncoupling of LCC-RyR on E-C coupling.

In the spatiotemporal 2D model, local $[Ca^{2+}]_i$ is elevated rapidly by Ca^{2+} influx (J_{LCC}) via an LCC and Ca^{2+} release flux (J_{RyR}) via a RyR cluster. The free Ca^{2+} diffuses according to the Fick's second Law, and is buffered by fluorescent indicator dye, troponin and calmodulin, and is withdrawn by SR Ca^{2+}-ATPase (J_{pump}) to SR and by Na^+/Ca^{2+} exchange (J_{NCX}) to extracellular matrix. The change of spatiotemporal free Ca^{2+} concentration ($[Ca^{2+}]_{i(x,y)}$) in the cytosol is given by equation (1):

$$\frac{\partial [Ca^{2+}]_{i(x,y)}}{\partial t} = D_x \frac{\partial^2 [Ca^{2+}]_{i(x,y)}}{\partial x^2} + D_y \frac{\partial^2 [Ca^{2+}]_{i(x,y)}}{\partial y^2} + J_{LCC}\delta(x_m, y_n) + J_{RyR}\delta(x_i, y_j) + \frac{d[Ca^{2+}]_{Trpn}}{dt} + \frac{d[Ca^{2+}]_{Cmdn}}{dt} + \frac{d[Ca^{2+}]_{dye}}{dt} + J_{leak} - J_{pump} + J_{NCX} \quad (1)$$

where $D_x = 0.30\ \mu m^2/ms$ and $D_y = 0.15\ \mu m^2/ms$, which are diffusion coefficients along x and y axes, respectively. J_{RyR} and J_{LCC} are the molar fluxes from RyR cluster and L-type channel. δ is the Dirac function, (x_m,y_n) is the location of L-type Ca^{2+} channel and (x_i,y_j) is that of RyR cluster, and m and n (i and j) are row and column indexes of a certain LCC (RyR). J_{leak} is a Ca^{2+} leak from SR to balance J_{pump} at the resting $[Ca^{2+}]_i$. J_{pump} is the pump flux by SR Ca^{2+} ATPase, and J_{NCX} is Na^+-Ca^{2+} changer flux. $[Ca^{2+}]_{Trpn}$, $[Ca^{2+}]_{Cmdn}$ and $[Ca^{2+}]_{dye}$ are cytoplasmic Ca^{2+} concentrations buffered by troponin, calmodulin and exogenous fluorescent dye, respectively, which are described as following differential equations [19]:

$$\frac{d[Ca^{2+}]_{Trpn}}{dt} = -\alpha_{Trpn}\left([Trpn]_{tot} - \left[Ca^{2+}\right]_{Trpn}\right)[Ca^{2+}]_i + \beta_{Trpn}\left(\frac{1 + 2(1 - Force_{norm})}{3}\right)\left[Ca^{2+}\right]_{Trpn} \quad (2)$$

$$\frac{d[Ca^{2+}]_{Cmdn}}{dt} = -\alpha_{Cmdn}([Cmdn]_{tot} - [Ca^{2+}]_{Cmdn})[Ca^{2+}]_i + \beta_{Cmdn}\left[Ca^{2+}\right]_{Cmdn} \quad (3)$$

$$\frac{d[Ca^{2+}]_{dye}}{dt} = -\alpha_{dye}([dye]_{tot} - [Ca^{2+}]_{dye})[Ca^{2+}]_i + \beta_{dye}\left[Ca^{2+}\right]_{dye} \quad (4)$$

where the definition and value of buffer parameters are given in Table 1, and $Force_{norm}$ is the normalized force and is described in section 2.3. Detailed equations and model parameters can be found in the APPENDIX.

During a twitch, activation of RyRs is described as stochastic process and simulated by Monte Carlo method. The opening probability of RyR cluster per unit time is dependent on local cytosolic Ca^{2+} concentration

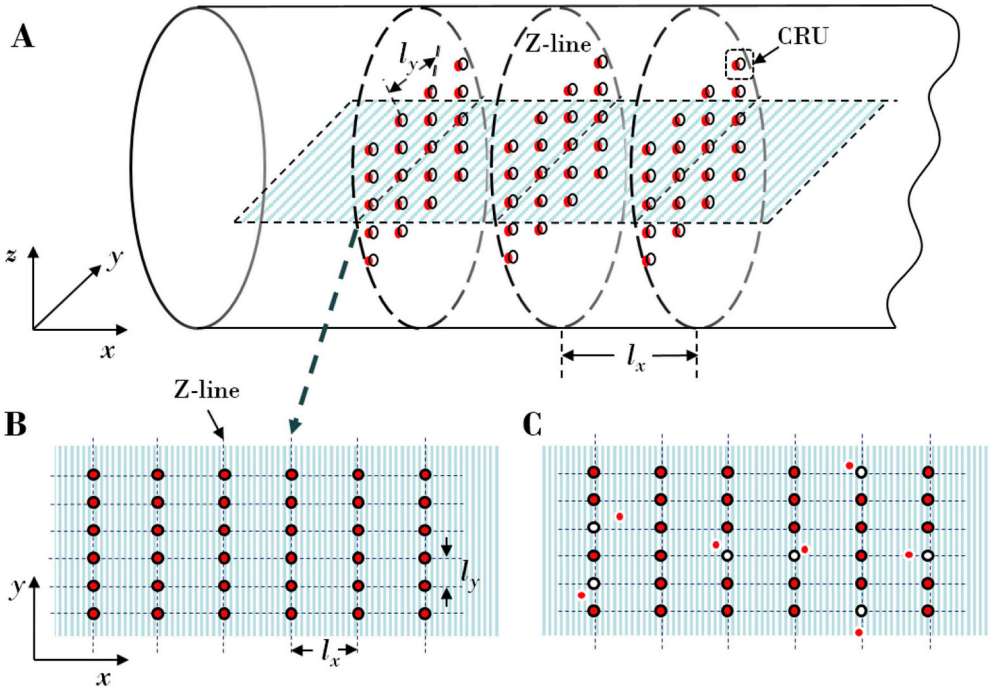

Fig. 1. Geometry of sub-cellular Ca^{2+} reaction-diffusion model. (A) Structural representation of a normal ventricular myocyte. Red dots are LCCs, and black rings are RyR clusters. lx = 2.0 μm, and ly = 1.0 μm. (B) 2-D geometry of CRUs network in the heathy heart, where LCCs and RyRs are overlapped in the same CRUs. (C) Irregular distribution of LCCs in heart failure, ~20% of LCCs are randomly rearranged here. (For interpretation of the references to colour in this figure legend, the reader is referred to the Web version of this article.)

Table 1
Ca^{2+} buffer Parameters.

Parameters	Definition	Value
$[Trpn]_{tot}$	Total cytosolic troponin centration	0.123 mM
α_{Trpn}	Binding rate of Ca^{2+} to troponin	100.0 $mM^{-1}ms^{-1}$
β_{Trpn}	Disassociation rate of Ca^{2+} to troponin	0.1 ms^{-1}
$[Cmdn]_{tot}$	Total cytosolic calmodulin centration	0.05 mM
α_{Cmdn}	Binding rate of Ca^{2+} to calmodulin	100.0 $mM^{-1}ms^{-1}$
β_{Cmdn}	Disassociation rate of Ca^{2+} to calmodulin	0.5 ms^{-1}
$[dye]_{tot}$	Total cytosolic fluorescent dye centration	0.05 mM
α_{dye}	Binding rate of Ca^{2+} to fluorescent dye	80.0 $mM^{-1}ms^{-1}$
β_{dye}	Disassociation rate of Ca^{2+} to fluorescent dye	0.09 ms^{-1}

($[Ca^{2+}]_{i\ (x,y)}$) and luminal Ca^{2+} concentration ($[Ca^{2+}]_{SR}$). It can be written as [16]:

$$P_{RyR(x_i,y_j)} = \frac{P_{max}}{1 + (K_m/[Ca^{2+}]_{i(x,y)})^n} \cdot \frac{k_{max}}{1 + \left(D_{SR}/[Ca^{2+}]_{SR}\right)^{n_{SR}}} \tag{5}$$

where $P_{max} = 0.303$/RyR cluster/ms, $k_{max} = 2.0$, the Hill coefficient $n_{SR} = 4.5$, $n = 1.6$, K_m is the cytoplasmic Ca^{2+} sensitivity parameter of RyR cluster, and D_{SR} is the luminal Ca^{2+} sensitivity parameter of Ca^{2+} release events. As reported, in HF, RyRs became unstable and oversensitive to cytoplasmic Ca^{2+} as well as SR luminal Ca^{2+} concentration [21–23]. In the simulation, the value of K_m was reduced from 15 μM in normal ventricular cell to 7.5 μM in failing myocyte, D_{SR} was 3.25 mM for normal heart and 2.75 mM for failing heart [16].

2.2. Electrophysiological model

Every AP at the frequency of 1 Hz is initiated by an external stimulus current I_{stim} with the duration of 1 ms and an amplitude of −38 pA/pF. The change of membrane voltage (V_m) can be described with the following differential equation:

$$\frac{dV_m}{dt} = -\frac{1}{C_m}(I_{Na} + I_{LCC} + I_{to} + I_{Kr} + I_{Ks} + I_{K1} + I_{NaK} + I_{NCX} + I_{pCa} + I_{pK} + I_{bCa} + I_{bNa} + I_{stim}) \tag{6}$$

where C_m is the cell membrane capacitance per unit surface area, I_{Na} is Na^+ current, I_{LCC} is the L-type Ca^{2+} current, I_{to} is the transient outward current, I_{Kr} is the rapid delayed rectifier current, I_{Ks} is the slow delayed rectifier current, I_{K1} is the inward rectifier K^+ current, I_{NaK} is the Na^+/K^+ pump current, I_{NCX} is the Na^+/Ca^{2+} exchanger current, I_{pCa} and I_{pK} are plateau Ca^{2+} and K^+ currents, and I_{bCa} and I_{bK} are background Ca^{2+} and K^+ currents (see APPENDIX for details). The ionic currents across the sarcolemma are based on the model by ten Tusscher et al. [24]. Changes of some ionic currents and Ca^{2+} related proteins have been observed in failing heart [25–28]. Modified parameters used in our HF model are shown in Table 2.

Ca^{2+} cycling system plays a key role in connecting the 2-D Ca^{2+} reaction-diffusion system and the cellular contraction. The L-type Ca^{2+} current I_{LCC} and SR release current I_{rel} first flow into the subsarcolemmal subspace where LCCs and RyRs are colocalized, and then the free Ca^{2+} ions are transferred to the bulk cytoplasm via diffusive Ca^{2+} current I_{xfer}. Those cytoplasmic Ca^{2+} ions are pumped back to SR via I_{up} and transferred out of the cell via I_{NCX}. Subspace free Ca^{2+} concentration ($[Ca^{2+}]_{ss}$), global free Ca^{2+} concentration ($[Ca^{2+}]_i$), and total Ca^{2+} concentration in the SR ($[Ca^{2+}]_{SRtotal}$) are formulated as follows:

$$\frac{d[Ca^{2+}]_{ss}}{dt} = I_{rel}\frac{V_{sr}}{V_{ss}} - I_{xfer}\frac{V_c}{V_{ss}} - \frac{I_{LCC}}{2V_{ss}F} + \frac{d[Ca^{2+}]_{ssbuf}}{dt} \tag{7}$$

$$\frac{d[Ca^{2+}]_i}{dt} = I_{xfer} - \frac{I_{bCa} + I_{pCa} - 2I_{NCX}}{2V_cF} + \frac{V_{SR}}{V_c}(I_{leak} - I_{up}) + \frac{d[Ca^{2+}]_{Trpn}}{dt} + \frac{d[Ca^{2+}]_{Cmdn}}{dt} + \frac{d[Ca^{2+}]_{dye}}{dt} \tag{8}$$

$$\frac{d[Ca^{2+}]_{SRtotal}}{dt} = I_{up} - I_{leak} - I_{rel} \tag{9}$$

$$[Ca^{2+}]_{SRbuf} = \frac{[Ca^{2+}]_{SR} \times Buf_{SR}}{[Ca^{2+}]_{SR} + K_{bufSR}} \tag{10}$$

$$I_{xfer} = V_{xfer}([Ca^{2+}]_{ss} - [Ca^{2+}]_i) \tag{11}$$

$$I_{rel} = V_{rel}O([Ca^{2+}]_{SR} - [Ca^{2+}]_{ss}) \tag{12}$$

where O is the proportion of opening RyR clusters to all RyR clusters in the 2-D subcellular model. $[Ca^{2+}]_{ssbuf}$ is the buffered subspace Ca^{2+} concentration, and $[Ca^{2+}]_{SRbuf}$ is the buffered SR Ca^{2+} concentration. $[Ca^{2+}]_{SR}$ is the free Ca^{2+} in the SR, and $[Ca^{2+}]_{SRtotal} = [Ca^{2+}]_{SRbuf} + [Ca^{2+}]_{SR}$. Detailed equations and parameters are shown in APPENDIX.

2.3. Contraction model

We incorporate the force computation equations in the model by Rice et al. [33] and Iribe et al. [19] into our model as follows:

$$Force = \zeta Force_{norm} \tag{13}$$

$$Force_{norm} = \frac{\phi_{SL}(P1 + N1 + 2P2 + 3P3)}{Force_{max}} \tag{14}$$

where $\zeta = 0.1$ N/m^2 is the conversion factor for normalization to physiological force. Φ_{SL} is the sarcomere overlap ratio, which equals to 1.0 when sarcomere length is 2.0 μm. P1, P2, P3 and N1 are referred to fractions of functional units in the respective force-generating states. In detail, Pi(i = 1,2,3) denotes the state of permissive tropomyosin with i cross bridges, N1 is the state of non-permissive tropomyosin with 1 cross bridge. $Force_{max}$ is the maximum force caused by an entire activation of tropomyosin. A detailed list of all equations and parameters can be found in the APPENDIX.

2.4. Numerical methods

The ordinary differential equations and partial differential

Table 2
Parameters in nonfailing and failing myocyte models.

Parameters	Definition	Nonfailing	Failing	References
V_{max}	Maximal SR Ca^{2+} pumping rate	0.006375 mM/ms	0.004144 mM/ms	[25]
G_{Ks}	Maximal I_{Ks} conductance	0.392 nS/pF	0.196 nS/pF	[27]
G_{K1}	Maximal I_{K1} conductance	5.405 nS/pF	4.324 nS/pF	[26,29]
G_{to}	Maximal I_{to} conductance	0.294 nS/pF	0.185 nS/pF	[30]
G_{Na}	Maximal I_{Na} conductance	14.84 nS/pF	8.902 nS/pF	[28]
P_{NaK}	Maximal I_{NaK}	2.724 pA/pF	1.57 pA/pF	[31]
G_{bCa}	Maximal I_{bCa} conductance	0.000592 nS/pF	0.0009054 nS/pF	[16]
k_{NCX}	Maximal I_{NCX}	1000 pA/pF	1500 pA/pF	[7,32]

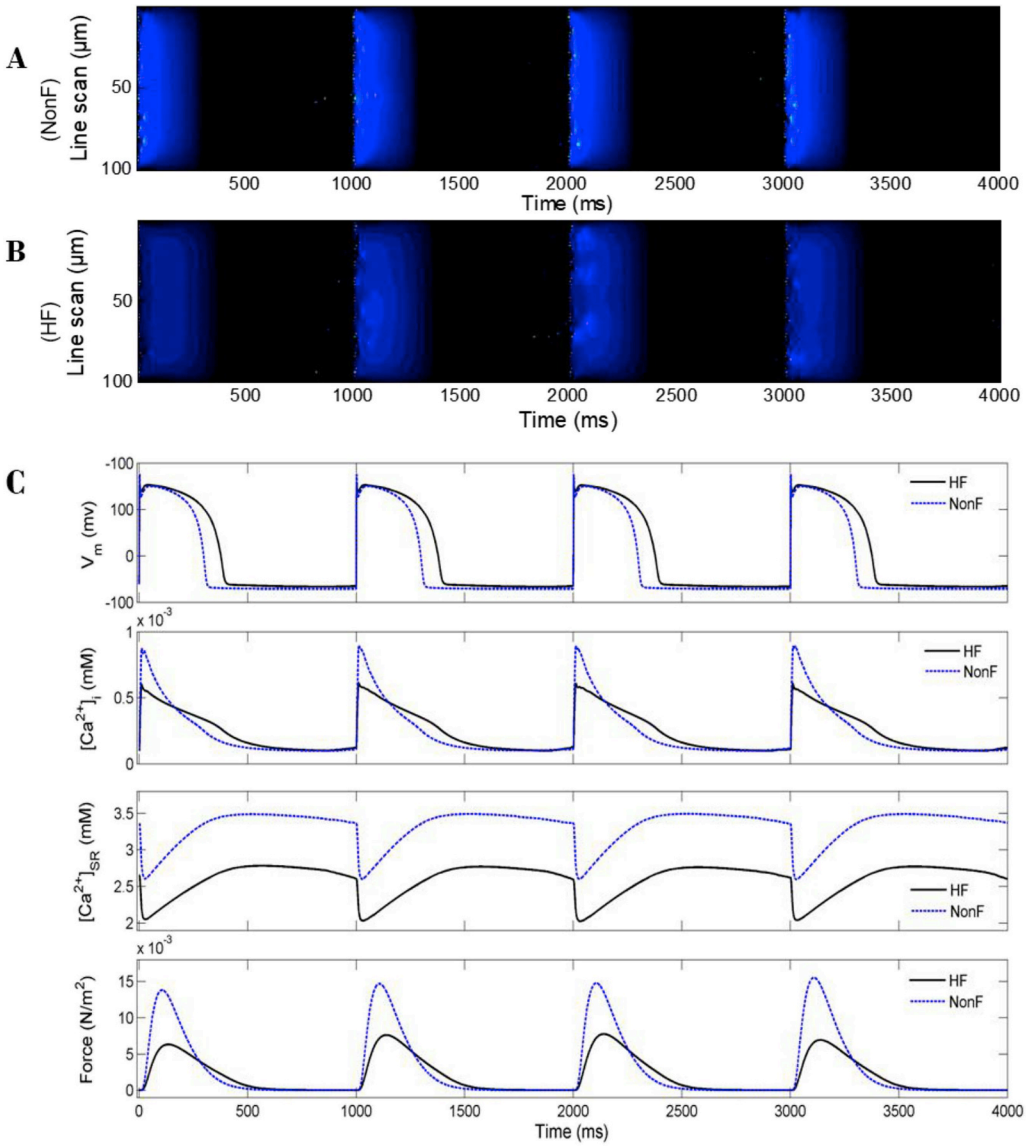

Fig. 2. Simulation results of Ca^{2+} dynamics, electrophysiology and contraction in nonfailing heart (NonF) vs. heart failure (HF). (A) and (B) Line-scan images along longitudinal direction of the cell in nonfailing and failing heart, respectively. (C) Curves of membrane potential (V_m), cytoplasmic Ca^{2+} concentration ($[Ca^{2+}]_i$), SR luminal Ca^{2+} concentration ($[Ca^{2+}]_{SR}$) and isometric force (Force) from failing heart (black solid lines) and nonfailing heart (blue dash lines). (For interpretation of the references to colour in this figure legend, the reader is referred to the Web version of this article.)

equations of diffusion are approximated by the finite difference method (FDM). The forward difference formula is used for the derivative with respect to t with a time-step $\Delta t = 0.01$ ms, and central difference formula for that with respect to x and y with mesh size of 0.1 μm. All averaged data is presented as mean $\pm$ SEM (n = 12). One-way analysis of variance (ANOVA) is used for comparison and $P < 0.05$ is accepted as statistical significance.

3. Results

3.1. Simulation results with intact coupling of LCC-RyRs

As shown in Fig. 2, spatiotemporal Ca^{2+} reaction-diffusion process and electrical-mechanical activities were simultaneously traced by our multiscale model in nonfailing and failing myocytes. In HF simulation, changes of some ionic currents and Ca^{2+} related proteins are shown in Table 2 without redistribution of LCCs. While the longitudinal line-scan image at $y = 10$ μm exhibits a bright $[Ca^{2+}]_i$ transient in nonfailing ventricular cell (Fig. 2(A)), the line-scan image at the same plane in failing myocyte shows a darker but slower decaying transient (Fig. 2(B)). Due to the unbroken coupling of LCC-RyRs, once a cell is stimulated, almost all the sparks are triggered synchronously by the depolarization-activated I_{LCC} in both line-scan images.

In Fig. 2(C), black solid curves obtained under heart failure conditions are different from the blue dash curves under nonfailing conditions, resulting from impaired Ca^{2+} handling and modified ion channels. Compared with that in nonfailing cells, action potential from HF shows a lower depolarization amplitude (88% of NonF amplitude), a higher resting potential (increment of 2–3 mV), and a larger and broader plateau that causing an increase in AP duration (APD_{90} in HF is 27% longer). Due to upregulation of I_{NCX} and reduced pumping rate of SR Ca^{2+} ATPase in HF, more Ca^{2+} ions are extruded from SR Ca^{2+} store to extracellular matrix, so that $[Ca^{2+}]_{SR}$ is unloaded by about 20%. Furthermore, both global intracellular $[Ca^{2+}]_i$ and isometric force in HF exhibit significant decrease in amplitude and slowed decay. Those curves in both normal and HF cells show a beat to beat fluctuation that results from stochastic property of activation of RyR release channels. For 12 repeated twitches, the amplitude of $[Ca^{2+}]_i$ is reduced by

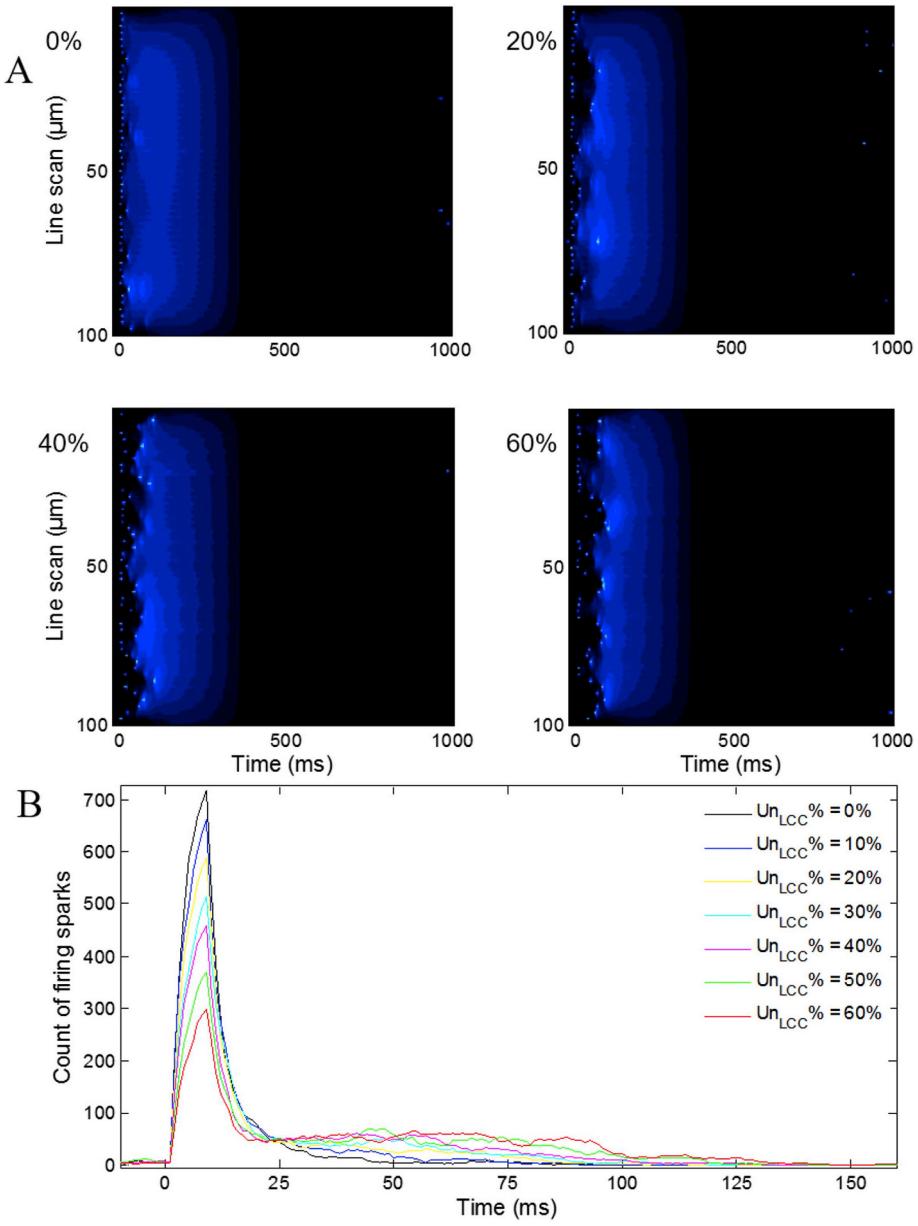

Figure 3. (A) line-scan images along longitudinal direction of the failing cell during a Ca^{2+} transient with uncoupled LCCs from 0% to 60%. (B) The counts of Ca^{2+} sparks in the activated state in a Ca^{2+} transient for different Un_{LCC}% from 0% to 60%.

31.2 ± 0.4%, from 0.890 ± 0.002 μM in nonfailing cell to 0.612 ± 0.002 μM in HF. The peak of force decreases by 50.5 ± 1.9%, from 0.0147 ± 0.0002 N/m^2 in nonfailing cell to 0.0073 ± 0.0002 N/m^2 in failing myocyte. The decay time of $[Ca^{2+}]_i$ from the peak to 90% reduction (T_{Ca90}) is 351.2 ± 1.0 ms in normal heart, while T_{Ca90} is prolonged by 45%–508.1 ± 0.7 ms in HF. The decay time of force (T_{F90}) is also increased by 37%, from 260.3 ± 0.2 ms in healthy heart to 355.6 ± 1.5 ms in failing heart.

3.2. Uncoupling of LCC-RyR leads to defective EC coupling

To investigate the relationship between remodelling of CRU microstructure and Ca^{2+} dynamics, a percentage of LCCs were rearranged randomly within the sarcomere. Fig. 3(A) shows line-scan images along *x* direction at y = 10 μm for one twitch when Un_{LCC}% is 0%,20%, 40%, and 60%, respectively. The firings of Ca^{2+} sparks become more and more dyssynchronous along with more uncoupled LCCs. In Fig. 3(B) the numbers of RyR clusters in the activated state (as the form of sparks) are counted per time (ms) for different Un_{LCC}% ranging from 0% to 60%. Those curves show that a number of sparks are intensively activated in the first 20 ms, which are initiated directly by inward Ca^{2+} current via LCCs colocalized in the same CRUs. It is worth noting that as the percentage of uncoupled LCCs increases, the peak number of sparks decreases, but more sparks were fired in the following 80–90 ms. These results suggest the positive relationship between dyssynchrony of Ca^{2+} sparks and the uncoupled LCCs.

Furthermore, 12 APs were simulated and averaged for each value of Un_{LCC}% to get statistical results in consideration of the stochastic properties of rearrangement of uncoupled LCCs and activation of RyR channels. Fig. 4(A) shows that as the percentage of uncoupled LCCs increases from 0% to 60%, while the initial peak of $[Ca^{2+}]_i$ is decayed gradually, a prominent peak appears later, which may be caused by the dyssynchronously firing of Ca^{2+} sparks in Fig. 3. In Fig. 4(B), the peaks of force curves are delayed but the shapes are similar. The times needed to reach the peak of $[Ca^{2+}]_i$ (T_{Capeak}) were recorded and averaged (n = 12) with different Un_{LCC}% in Fig. 4(C). The times taken to reach

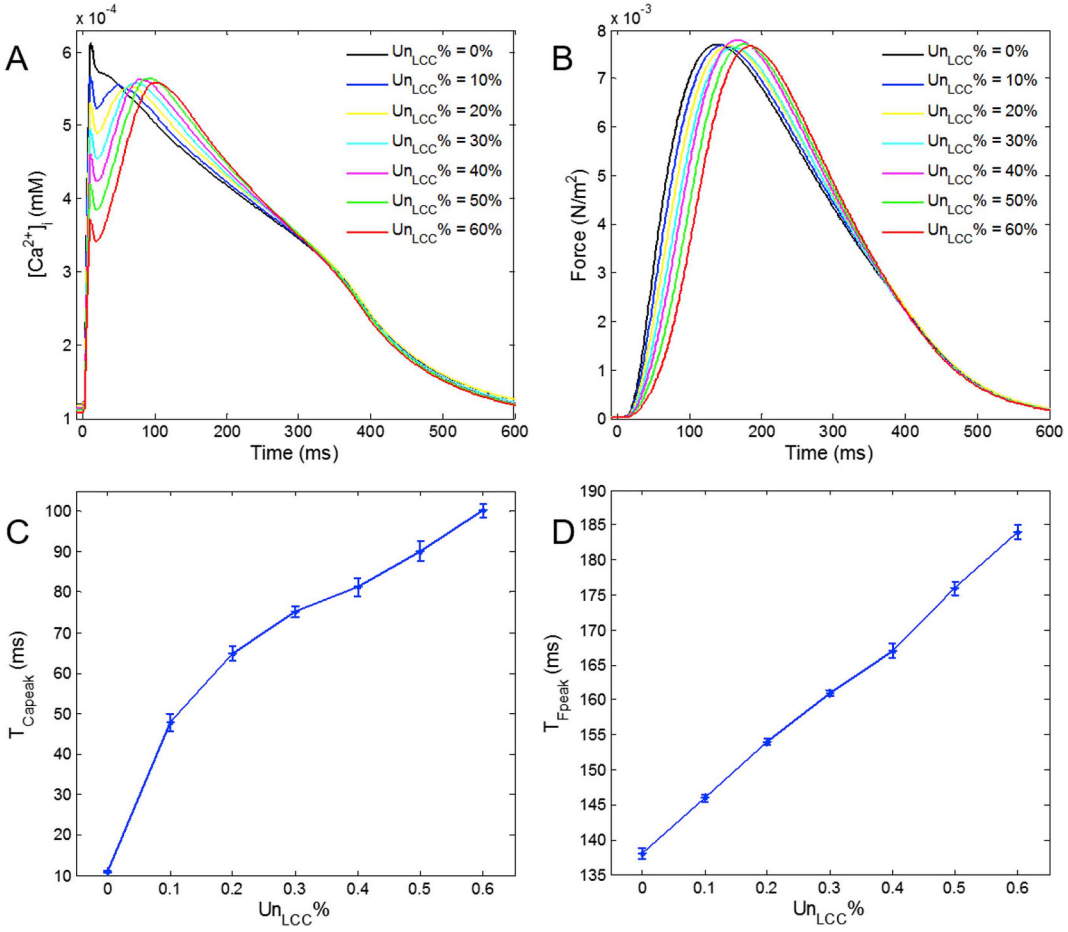

Fig. 4. Effects of uncoupled LCC-RyR on Ca^{2+} handling and contraction. (A) Seven curves of averaged intracellular $[Ca^{2+}]_i$ in failing ventricular myocyte when $Un_{LCC}\%$ = 0%–60%. (B) Corresponding curves of isometric contractile force. (C) and (D) The dependence of T_{Capeak} and T_{Fpeak} on the fraction of rearranged LCCs. T_{Capeak} is the time from the starting of external stimulus to the peak of global $[Ca^{2+}]_i$ and T_{Fpeak} is the time to the peak value of force.

the maximum value of forces (T_{Fpeak}) were shown in Fig. 4(D). When $Un_{LCC}\%$ is upregulated from 20% to 60% by a step of 10%, T_{Capeak} is increased gradually from 64.8 ± 1.7 ms to 100.2 ± 1.6 ms by a step of approximately 10 ms ($p < 0.05$), and T_{Fpeak} is extended from 154.2 ± 0.4 ms to 184.3 ± 1.0 ms by an augment of 6–8 ms ($p < 0.05$). These findings imply that the uncoupling of LCC-RyR may play a role in remodelling the heartbeats, causing a moderate deceleration of systolic process.

3.3. The importance of the uncoupling degree

Although the remodelling of TTs was found in heat failure [18], we further investigated the effect of the redistribution of LCCs in normal cells by using the proposed model. Similar to the results in HF conditions, delays of the time to peak of both calcium transients and contraction forces were also observed by uncoupling the LCC-RyRs couplons with different $Un_{LCC}\%$ (see Appendix, Fig. S2). These findings imply the importance of LCC-RyR coupling in both normal and HF cells.

There are two sources of randomness, randomness in the timing course of CRU release events and randomness in the distribution of the LCCs, in our model. The firing of CRU release events is a stochastic process that is implemented by using Monte Carlo method as many other researchers did [20,34]. The effect of randomness of LCCs redistribution was studied by comparing simulations with fixed and random LCCs redistributions as shown in Fig. 5. Comparing with the cases of fixed LCCs redistribution, the statistical results of the random LCC redistribution show insignificant differences ($p > 0.05$) (Fig. 5). It suggests that the uncoupling degree (the variable $Un_{LCC}\%$ in our work) but not the randomness of LCC redistribution plays an important role in disordered Ca^{2+} handling and contractile force in HF.

4. Discussion

In our simulation, failing ventricular myocyte is characterized by prolonged AP duration, unloaded SR Ca^{2+} store, decreased Ca^{2+} transient, and impaired contractile force. Uncoupling of LCC-RyRs would further perturb Ca^{2+} handling. Experimental observations have showed that the dyssynchronous Ca^{2+} release and reorganization or the regional loss of TTs should be one of the major causes of heart failure [18,35,36]. Our simulation demonstrates that stray LCCs decoupled with RyRs in the CRUs are largely responsible for the dyssynchronous Ca^{2+} sparks. With more LCCs leaving their original locations, more RyRs are spatially isolated and unable to be triggered when initial Ca^{2+} enters via depolarization-activated LCCs. Those Ca^{2+} release channels would, however, be activated with a delay when the local Ca^{2+} concentration is elevated by diffusive Ca^{2+} wave propagating from preceding activated Ca^{2+} sparks nearby. Therefore, the amount of calcium release is almost the same yet shows a delay correlating to the percentage of uncoupling. The force is calculated from the global calcium concentration after diffusing and buffering of calcium release events and the curves show insignificant changes in amplitude yet a delay to reach the peaks.

Compared with failing cells with intact coupling of LCC-RyRs, the simulation of the failing myocytes with uncoupling of LCC-RyRs has not only shown the dyssynchronous Ca^{2+} sparks but also worse Ca^{2+} transient and delayed isomeric force. With the same cytoplasmic

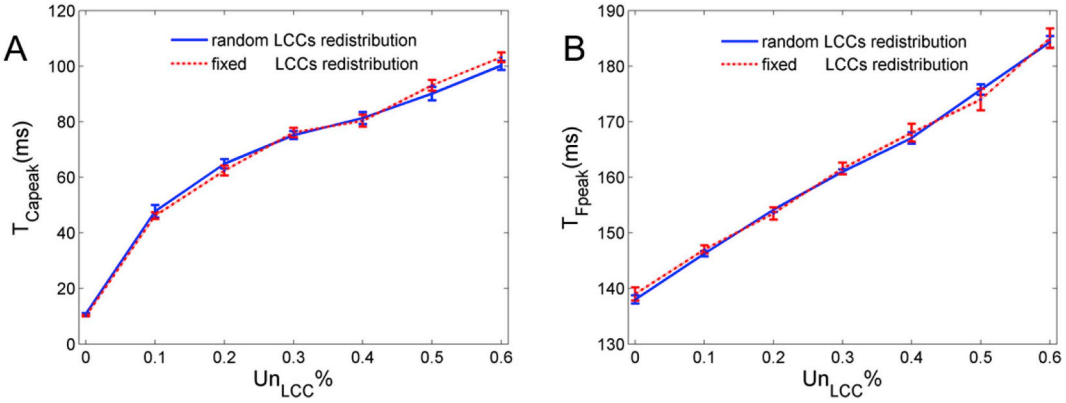

Fig. 5. The dependence of T_{Capeak} and T_{Fpeak} on the ratios of redistributed LCCs. The blue curve is calculated from 12 cardiac cycles with random LCC redistribution, and the red curve is with fixed LCC redistribution. (For interpretation of the references to colour in this figure legend, the reader is referred to the Web version of this article.)

buffering system and contraction model, the values of isomeric force peaks are affected slightly by the dyssynchrony due to the almost unaltered total amount of Ca^{2+} release. However, the time to reach the force peak (T_{Fpeak}) is prolonged gradually with larger fraction of repositioned LCCs. For example, when 20% of LCCs were rearranged randomly, ΔT_{Fpeak} is about 16 ms, and for 30% of rearranged LCCs, ΔT_{Fpeak} is about 23 ms. It seems that a moderate uniform remodelling of TTs over the ventricle might not have severe effect on the cardiac contractility under the HF conditions. However, with the occurrence of progressive remodelling of TTs, ΔT_{Fpeak} is near 50 ms for 60% of uncoupled LCC-RyRs, which may practically alter the systolic process. Furthermore, it was reported that spatial heterogeneity of cardiac electrophysiology might be an important mechanism for ventricular arrhythmias [37]. Similarly, if inhomogeneous remodelling occurs within ventricular tissue, systolic synchrony and pumping efficiency of whole ventricle is likely to be impaired due to various latencies of myocyte force.

Besides progressive pump failure, a lethal arrhythmia is thought to be a major cause to sudden cardiac death in patients with severe HF [26,38]. Our further work would focus on the underlying relationship between remodelling of Ca^{2+} relevant proteins or structures and arrhythmias.

5. Summary

Our study has demonstrated that a subcellular structural alteration would probably impair the efficiency of E-C coupling and physiological function of a failing heart. This attempt proposes a better understanding of the Ca^{2+} handling and electro-mechanical properties in failing heart, and would be beneficial for therapeutic treatments against heart failure.

Authors' contributions

This work is the product of intellectual work of the whole team. Research concept, writing of the manuscript: XZ, LL. The analytical methods used, simulation design, simulation source code: LL. Simulation process and data analysis: QZ. Writing-review and editing: LX. All authors read and approved the final manuscript.

Conflicts of interest

The authors declare that they have no conflict of interests.

Acknowledgments

The authors would like to thank Dr Lingyan Shi, Department of Chemistry, Columbia University, for her valuable suggestions and English language assistance in preparing manuscript.

Appendix A. Supplementary data

Supplementary data to this article can be found online at https://doi.org/10.1016/j.compbiomed.2019.04.007.

Funding

This work was supported by National Natural Science Foundation of China (61302130), Wenzhou Municipal Science and Technology Bureau (G20150022), and Research Funds of Wenzhou Medical University (QTJ14018, QTJ14010).

References

[1] C.C. Yin, F.A. Lai, Intrinsic lattice formation by the ryanodine receptor calcium-release channel, Nat. Cell Biol. 2 (9) (2000) 669–671.
[2] Shi Qiang, M.D.S. Wang, Eduardo Ríos, Heping Cheng, The quantal nature of Ca2+ sparks and in situ operation of the ryanodine receptor array in cardiac cells, Proc. Natl. Acad. Sci. U. S. A 101 (11) (2004) 3979.
[3] H. Cheng, W.J. Lederer, M.B. Cannell, Calcium sparks: elementary events underlying excitation-contraction coupling in heart muscle, Science 262 (5134) (1993) 740–744.
[4] S.Q. Wang, L.S. Song, E.G. Lakatta, H. Cheng, Ca2+ signalling between single L-type Ca2+ channels and ryanodine receptors in heart cells, Nature 410 (6828) (2001) 592–596.
[5] C. Franzini-Armstrong, F. Protasi, V. Ramesh, Shape, size, and distribution of Ca (2+) release units and couplons in skeletal and cardiac muscles, Biophys. J. 77 (3) (1999) 1528–1539.
[6] D.W. Baker, D. Einstadter, C. Thomas, R.D. Cebul, Mortality trends for 23,505 Medicare patients hospitalized with heart failure in Northeast Ohio, 1991 to 1997, Am. Heart J. 146 (2) (2003) 258–264.
[7] K.R. Sipido, P.G. Volders, M.A. Vos, F. Verdonck, Altered Na/Ca exchange activity in cardiac hypertrophy and heart failure: a new target for therapy? Cardiovasc. Res. 53 (4) (2002) 782–805.
[8] A.J. Lokuta, P.A.N. Maertz, S.V. Meethal, T.K. Potter, T.J. Kamp, H.H. Valdivia, et al., Increased nitration of sarcoplasmic reticulum Ca2+-ATPase in human heart failure, Circulation 111 (111) (2005) 988–995.
[9] A. Muller, W.S. Simonides, Regulation of myocardial SERCA2a expression in ventricular hypertrophy and heart failure, Future Cardiol. 1 (4) (2005) 543–553.
[10] T.R. Shannon, S.M. Pogwizd, D.M. Bers, Elevated sarcoplasmic reticulum Ca2+ leak in intact ventricular myocytes from rabbits in heart failure, Circ. Res. 93 (7) (2003) 592–594.
[11] J. Fauconnier, A. Lacampagne, J.M. Rauzier, G. Vassort, S. Richard, Ca2+-dependent reduction of Ik1 in rat ventricular cells: a novel paradigm for arrhythmia in heart failure? Cardiovasc. Res. 68 (2) (2005) 204–212.
[12] G. Santulli, W. Xie, S.R. Reiken, A.R. Marks, Mitochondrial calcium overload is a key determinant in heart failure, Proc. Natl. Acad. Sci. U. S. A 112 (36) (2015) 11389–11394.
[13] A. Kiarash, C.E. Kelly, B.S. Phinney, H.H. Valdivia, J. Abrams, S.E. Cala, Defective glycosylation of calsequestrin in heart failure, Cardiovasc. Res. 63 (2) (2004) 264–272.
[14] S. Jacob, N.H. Sleiman, S. Kern, L.R. Jones, J.A. Sala-Mercado, T.P. McFarland,

H.H. Sabbah, S.E. Cala, Altered calsequestrin glycan processing is common to diverse models of canine heart failure, Mol. Cell. Biochem. 377 (1–2) (2013) 11–21.
[15] L. Lu, L. Xia, X. Ye, H. Cheng, Simulation of the effect of rogue ryanodine receptors on a calcium wave in ventricular myocytes with heart failure, Phys. Biol. 7 (2) (2010) 026005.
[16] L. Lu, L. Xia, X. Zhu, Simulation of arrhythmogenic effect of rogue RyRs in failing heart by using a coupled model, Comput. Math. Methods Med. 2012 (2012) (2012) 183978.
[17] E.A. Sobie, S. Guatimosim, L. Gomez-Viquez, L.S. Song, H. Hartmann, M. Saleet Jafri, W.J. Lederer, The Ca 2+ leak paradox and rogue ryanodine receptors: SR Ca 2+ efflux theory and practice, Prog. Biophys. Mol. Biol. 90 (1–3) (2006) 172–185.
[18] L.S. Song, E.A. Sobie, S. McCulle, W.J. Lederer, C.W. Balke, H. Cheng, Orphaned ryanodine receptors in the failing heart, Proc. Natl. Acad. Sci. U. S. A. 103 (11) (2006) 4305–4310.
[19] G. Iribe, P. Kohl, D. Noble, Modulatory effect of calmodulin-dependent kinase II (CaMKII) on sarcoplasmic reticulum Ca2+ handling and interval–force relations: a modelling study, Philos. Trans. Roy. Soc. A Math. Phys. Eng. Sci. 364 (364) (2006) 1107–1133.
[20] L.T. Izu, W.G. Wier, C.W. Balke, Evolution of cardiac calcium waves from stochastic calcium sparks, Biophys. J. 80 (1) (2001) 103–120.
[21] S.E. Lehnart, X.H. Wehrens, A.R. Marks, Calstabin deficiency, ryanodine receptors, and sudden cardiac death, Biochem. Biophys. Res. Commun. 322 (4) (2004) 1267–1279.
[22] X. Ai, J.W. Curran, T.R. Shannon, D.M. Bers, S.M. Pogwizd, Ca2+/calmodulin-dependent protein kinase modulates cardiac ryanodine receptor phosphorylation and sarcoplasmic reticulum Ca2+ leak in heart failure, Circ. Res. 97 (12) (2005) 1314–1322.
[23] S. Nattel, A. Maguy, S. Le Bouter, Y.H. Yeh, Arrhythmogenic ion-channel remodeling in the heart: heart failure, myocardial infarction, and atrial fibrillation, Physiol. Rev. 87 (2) (2007) 425–456.
[24] K.H. ten Tusscher, A.V. Panfilov, Alternans and spiral breakup in a human ventricular tissue model, Am. J. Physiol. Heart Circ. Physiol. 291 (3) (2006) H1088–H1100.
[25] R.H. Schwinger, M. Bohm, U. Schmidt, P. Karczewski, U. Bavendiek, M. Flesch, E.G. Krause, E. Erdmann, Unchanged protein levels of SERCA II and phospholamban but reduced Ca2+ uptake and Ca(2+)-ATPase activity of cardiac sarcoplasmic reticulum from dilated cardiomyopathy patients compared with patients with nonfailing hearts, Circulation 92 (11) (1995) 3220–3228.
[26] G.F. Tomaselli, D.P. Zipes, What causes sudden death in heart failure? Circ. Res. 95 (8) (2004) 754–763.
[27] G.R. Li, C.P. Lau, A. Ducharme, J.C. Tardif, S. Nattel, Transmural action potential and ionic current remodeling in ventricles of failing canine hearts, Am. J. Physiol. Heart Circ. Physiol. 283 (3) (2002) H1031–H1041.
[28] C.R. Valdivia, W.W. Chu, J. Pu, J.D. Foell, R.A. Haworth, M.R. Wolff, T.J. Kamp, J.C. Makielski, Increased late sodium current in myocytes from a canine heart failure model and from failing human heart, J. Mol. Cell. Cardiol. 38 (3) (2005) 475–483.
[29] D.J. Beuckelmann, M. Nabauer, E. Erdmann, Alterations of K+ currents in isolated human ventricular myocytes from patients with terminal heart failure, Circ. Res. 73 (2) (1993) 379–385.
[30] M. Nabauer, D.J. Beuckelmann, P. Uberfuhr, G. Steinbeck, Regional differences in current density and rate-dependent properties of the transient outward current in subepicardial and subendocardial myocytes of human left ventricle, Circulation 93 (1) (1996) 168–177.
[31] O.I. Shamraj, I.L. Grupp, G. Grupp, D. Melvin, N. Gradoux, W. Kremers, J.B. Lingrel, A. De Pover, Characterisation of Na/K-ATPase, its isoforms, and the inotropic response to ouabain in isolated failing human hearts, Cardiovasc. Res. 27 (12) (1993) 2229–2237.
[32] G. Hasenfuss, W. Schillinger, S.E. Lehnart, M. Preuss, B. Pieske, L.S. Maier, J. Prestle, K. Minami, H. Just, Relationship between Na+-Ca2+-exchanger protein levels and diastolic function of failing human myocardium, Circulation 99 (5) (1999) 641–648.
[33] J.J. Rice, R.L. Winslow, W.C. Hunter, Comparison of putative cooperative mechanisms in cardiac muscle: length dependence and dynamic responses, Am. J. Physiol. 276 (5) (1999) H1734–H1754.
[34] C. Soeller, I.D. Jayasinghe, P. Li, A.V. Holden, M.B. Cannell, Three-dimensional high-resolution imaging of cardiac proteins to construct models of intracellular Ca2+ signalling in rat ventricular myocytes, Exp. Physiol. 94 (5) (2009) 496–508.
[35] S.E. Litwin, D. Zhang, J.H.B. Bridge, Dyssynchronous Ca2+ sparks in myocytes from infarcted hearts, Circ. Res. 87 (11) (2000) 1040.
[36] F.R. Heinzel, V. Bito, L. Biesmans, M. Wu, E. Detre, F.V. Wegner, P. Claus, S. Dymarkowski, F. Maes, J. Bogaert, Remodeling of T-tubules and reduced synchrony of Ca2+ release in myocytes from chronically ischemic myocardium, Circ. Res. 102 (3) (2008) 338–346.
[37] R.H. Clayton, A.V. Holden, Effect of regional differences in cardiac cellular electrophysiology on the stability of ventricular arrhythmias: a computational study, Phys. Med. Biol. 48 (1) (2003) 95–111.
[38] D.M. Roden, A surprising new arrhythmia mechanism in heart failure, Circ. Res. 93 (7) (2003) 589–591.